J. Physique **45** (1984) 191-206 FÉVRIER **1984**, PAGE 191

Classification
Physics Abstracts
03.65G — 63.00 — 71.00

Spectrum of harmonic excitations on fractals

R. Rammal (*)

Laboratoire de Physique de l'Ecole Normale Supérieure, 24, rue Lhomond, 75231 Paris, France

(*Reçu le 10 août 1983, accepté le 21 octobre 1983*)

Résumé. — La densité d'états et la nature des états propres d'un réseau de Sierpinski à d-dimensions sont étudiées. Les résultats obtenus sont valables aussi pour le modèle de liaisons fortes et pour tout hamiltonien quadratique. Pour $d > 1$, la mesure spectrale est la superposition de deux mesures purement ponctuelles, de poids relatifs $d/(d+1)$ et $1/(d+1)$. Les modes propres associés sont calculés explicitement. A la première partie du spectre sont associés des modes localisés avec des amplitudes non nulles seulement sur un nombre fini de sites (modes moléculaires), tandis que la seconde partie correspond à un nouveau type d'états : les modes hiérarchiques. L'influence des conditions aux limites est élucidée ainsi que l'importance de ce type de spectre en percolation quantique et pour les potentiels incommensurables.

Abstract. — The density of states and the nature of the eigenmodes of the vibrating d-dimensional Sierpinski gasket are investigated. The results hold for the tight-binding or any general quadratic Hamiltonian. For $d > 1$, the spectral measure is shown to be a superposition of two distinct pure point measures of relative weights $d/(d+1)$ and $1/(d+1)$. The eigenmodes associated with each part are explicitly calculated. The first part of the spectrum is associated with localized modes, with non zero amplitudes only on a finite number of sites (molecular modes), whereas the second part is associated with a new kind of states : the hierarchical modes. The influence of the boundary conditions is also elucidated as well as the importance of this kind of spectrum in quantum percolation and incommensurate potentials.

1. Introduction.

Many physical properties of a many-body system are closely related to the spectrum of the Schrödinger equation. Of particular interest for physical applications are the nature of the spectral measure (pure point, absolutely continuous), the behaviour of the wave functions (localized or extended, chaotic or non chaotic) and the topological feature of the spectrum (connected, band spectrum, Cantor spectrum). For instance, it is well-known that the energy spectrum of a free particle in a periodic potential consists of bands of extended eigenstates. On the other hand, randomness of the potential may in general create localized states, arising from destructive quantum interference caused by the random potential. In addition, a localization-delocalization transition has been shown to exist (under special conditions) in almost periodic potentials (for instance for the « almost-Mathieu » equation [1]) in one dimension. In this paper we show that localization may occur also for non-random potentials on self-similar structures : deterministic fractals. In this respect, fractals may bridge the gap between crystalline structures and disordered materials. From a structural view point, it has been suggested [2] that fractals may represent the geometrical features of the percolation clusters. Very recently, this hint was confirmed by many authors [3], showing that percolating clusters are well-represented as fractal structures up to the percolation correlation length. However this example of fractals is not an isolated one. A linear or branched polymer, a random or self-avoiding walk in free space or on a periodic lattice are other examples of fractals. The common features of these structures in their dilation symmetry (scale invariance) in contrast with the translation symmetry possessed by standard Euclidean space.

In addition to the well-known fractal dimensionality [4] $\bar{d}$, the new concept of spectral dimensionality $\tilde{d}$ was introduced recently [5, 6] in order to describe the classical diffusion on fractals. It describes the low frequency density of states (e.g. for elastic vibrations) : $\rho(\omega) \sim \omega^{\tilde{d}-1}$. The dimensions $\bar{d}$ and $\tilde{d}$ also seem to control many other physical phenomena such as localization and self-avoidance of random walks. Euclidean spaces of dimension d are special and degenerate cases, because $\bar{d} = \tilde{d} = d$ in them.

(*) Permanent address : C.R.T.B.T., C.N.R.S., B.P. 166 X, 38042 Grenoble Cedex, France.

In this paper, we investigate the spectrum of the harmonic Hamiltonian on the d-dimensional Sierpinski gaskets. This family of self-similar structures can be built in any Euclidean dimension, and has been already applied in other studies [2, 7, 8] because it is particularly convenient for scaling computations.

In section 2, some definitions and appropriate notations are given. A renormalization procedure is used in this section in order to obtain the energy scaling relation associated with a spatial scaling. The recursion equation then obtained is used to calculate the spectral dimensionality $\tilde{d}$ as a function of d.

In section 3, we use another decimation scheme to calculate the energy spectrum of the gaskets. The set of iteration equations permit us to distinguish two parts in the spectrum. The first corresponds to a pure point spectral measure of relative weight $d/(d+1)$, supported by a set of Lebesgue measure zero. The second part, of relative weight $1/(d+1)$ is given by a Cantor spectrum of Lebesgue measure zero.

Section 4 is devoted to the eigenmode calculation. In particular, we show that the first part of the energy spectrum produces localized modes. The associated amplitudes, for these degenerate eigenmodes, are non zero only on a finite set of sites. The degree of localization is measured with one localization length, which diverges at the lower edge of the spectrum. The second part of the spectrum is associated with hierarchical states, having a hierarchy of localization lengths.

In section 5, the influence of the boundary conditions is discussed, and a comparison with other works is outlined.

2. Real space renormalization of the equations of motion.

2.1 SIERPINSKI GASKET. — The Sierpinski gaskets form a family of non trivial d-dimensional scale invariant fractal lattices of finite ramification order, but not quasi-one-dimensional [2, 4], which can be built in any Euclidean dimension. To construct a d-dimensional gasket, we begin with a d-dimensional hypertetrahedron G_0 (a triangle for $d = 2$) at stage $n = 0$. G_{n+1} is obtained from G_n by juxtaposition of $(d+1)$ stage n structures, at their external corners. The scaling factor is $b = 2$ at each iteration, and the fractal dimensionality of the gasket is easily found to be : $\bar{d} = \ln(d+1)/\ln 2$. The total number of sites at stage n is given by

$$N_n = (d+1)\,[1 + (d+1)^n]/2 \qquad (2.1)$$

and the corresponding number of edges is also given by

$$E_n = d[d+1]^{n+1}/2. \qquad (2.2)$$

A natural way to label the sites of the gasket consists in the use of p-adic numbers [9, 10]. These labels (see appendix II) are the « normal » coordinates on the gasket, playing a rôle similar to the Cartesian coordinates of Euclidean lattices. Each hypertetrahedron is coded with a p-adic number, and thus each site is labelled by a pair of such p-adic numbers. This method of coding is very useful in numerical simulation [11].

Assume now a system of N_n identical masses m placed at the sites of the gasket, and connected by springs of strength K. We make the simplification that particles are allowed to move only in a direction orthogonal to the d-dimensional space of the gasket. Let $\alpha = m\omega^2/K \equiv \omega^2/\omega_0^2$ denote the reduced squared frequency and $\{ U_j e^{i\omega t} \}$ the eigenstate associated with a mode of frequency ω. The set of equations of motion for sites i is given by

$$\alpha U_i = \sum_j (U_i - U_j) \qquad (2.3)$$

where j denotes a neighbouring site of i.

Equations like 2.3 occur also in other problems described by similar finite difference equations. For instance, in the tight-binding model for electrons on a lattice we have the same type of eigenvalue problems. In this case, the analogue of equation 2.3 is written

$$(E - \varepsilon)\,\psi_x = t \sum_{x'} \psi_{x'} \qquad (2.4)$$

where the energy at sites x is ε, ψ_x is the amplitude at site x, t is the hopping matrix element and E denotes the eigenvalue. The correspondence in this case is trivially given by the relation $(E-\varepsilon)/t \leftrightarrow 2d - \omega^2/\omega_0^2$. In general, equations analogous to 2.3 occur in the harmonic approximation. The method and the results of this paper hold then for a large class of models.

2.2 RENORMALIZATION OF THE COUPLING CONSTANT. — The self-similarity of the gasket leads to a natural decimation procedure. The idea involves eliminating in equation 2.2 the lowest scale amplitudes corresponding to the sites located at mid-point of hypetetrahedron edges. Then at each decimation, $(d+1)\,d/2$ sites are eliminated, and this procedure leads to a reduced set of equations describing the same physics on a gasket scaled down by a factor $b = 2$. This exact renormalization leads to a renormalized frequency (one parameter renormalization group). In the following we shall illustrate this procedure for $d = 2$, which gives directly the value of the spectral dimensionality $\tilde{d}$ (the general case is outlined in appendix I).

2.2.1 *Case* $d = 2$. — The set of equations of motion for the mid-points of the lowest left triangle (see Fig. 1) is :

$$\begin{aligned} \alpha x_1 &= 4x_1 - x_2 - x_3 - X_2 - X_3 \\ \alpha x_2 &= 4x_2 - x_1 - x_3 - X_1 - X_3 \\ \alpha x_3 &= 4x_3 - x_1 - x_2 - X_1 - X_2. \end{aligned} \qquad (2.5)$$

The corresponding equation for X_1 (or Z_1) is

$$\alpha X_1 = 4X_1 - (x_2 + x_3 + z_2 + z_3) \qquad (2.6)$$

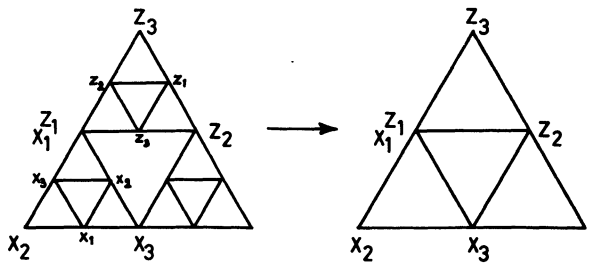

Fig. 1. — Principle of the decimation procedure, to derive the recursion relations for elastic vibrations on a two dimensional Sierpinski gasket.

Using equations 2.5, one extracts $x_2 + x_3$ as a function of $\{ X_i \}$ and the same for $z_2 + z_3$ as function of $\{ Z_i \}$. Inserting these values in equation 2.6, one obtains a new equation where X_1 is a function of X_2, X_3 and Z_2, Z_3. This relation can be cast in the form of the first equation 2.5 with the renormalization :

$$\alpha \to \alpha' = \alpha(5 - \alpha). \tag{2.7}$$

We note the absence of new coupling constants, in opposition to the case of Euclidean lattices. Given an eigenfrequency, this relation permits us to calculate the corresponding eigenstates from the equations relating $\{ x_i \}$ to $\{ X_i \}$. Keeping the strength K fixed, the result (2.7) can be understood as a mass renormalization :

$$m' = m(5 - m\omega^2/K). \tag{2.7'}$$

In particular, at low frequency ($\omega^2/\omega_0^2 \ll 5^{-n-1}$), after n iterations, the renormalized mass becomes $m_n \simeq 5^n.m$.

For the general d case, one obtains (see appendix I) the following result :

$$\alpha' \equiv \phi(\alpha) = \alpha(\delta - \alpha) \tag{2.8}$$

where $\delta = d + 3$.

2.2.2 *The spectral dimensionality* $\tilde{d}$. — The quadratic character of the map $\phi(\alpha) = \alpha(\delta - \alpha)$ obtained by the above decimation procedure is mainly due to the scaling by a factor $b = 2$ of the gasket. The whole spectrum of the gasket is controlled by the properties of the map ϕ, as we shall see below. In particular, the spectral dimensionality $\tilde{d}$ is given [6] by the slope of $\phi(\alpha)$ near its trivial fixed point $\alpha = 0$:

$$\tilde{d} \equiv \bar{d} \cdot \frac{2 \ln b}{|\ln \phi'(0)|} = 2 \ln (d + 1)/\ln (d + 3). \tag{2.9}$$

For example, $\tilde{d}$ reduces to the known-value $\tilde{d} = \bar{d} = 1$ at $d = 1$. The spectral dimensionality $\tilde{d}$ approaches monotonically its asymptotic value 2 at $d \gg 1$:

$$\tilde{d} = 2\left(1 - \frac{2/d}{\ln d} + \cdots\right) \tag{2.10}$$

whereas $\bar{d}$ reaches the value $\bar{d} = \infty$ at $d = \infty$. In table I, the values of $\bar{d}$ and $\tilde{d}$ are given for increasing values of the Euclidean dimension d. Notice that the inequalities : $\tilde{d} \leqslant \bar{d} \leqslant d$ are obeyed for all values of d.

A straightforward application of the above result is that excitations having

$$\rho(\omega) \sim \omega^{\tilde{d}-1} \tag{2.11}$$

as low frequency density of states produce the power law (Bosons) : $C(T) \sim T^{\tilde{d}}$ for the specific heat at low temperature ($T \ll \omega_0$). Similarly, for free particles of energy $\varepsilon \sim \omega^2$, we have the low energy density of states

$$n(\varepsilon) \sim \varepsilon^{\tilde{d}/2-1} \tag{2.12}$$

giving rise to a specific heat $C(T) \sim T^{\tilde{d}/2}$ at low temperature. In addition to this example, the relative value of $\tilde{d}$ governs the physical behaviours of the gasket [6] (and of fractals in general). For instance, Bose-Einstein condensation cannot take place for particles having (2.12) as density of states, if $\tilde{d} \leqslant 2$. The same ideas hold also for the ferromagnetic spherical model. More generally, $\tilde{d}$ controls the infrared catastrophe and the critical behaviour of non Ising spin models where spins are located on fractals.

Table I.

d	$\tilde{d}$	$\bar{d}$
1	1	1
2	1.364	1.584
3	1.547	2
4	1.653	2.321
5	1.723	2.584
6	1.771	2.808
∞	2	∞

2.2.3 *On the nature of the map* $\phi(\alpha)$. — In general $\phi(\alpha)$ is a rational function (see Eq. A.8 in the appendix) of α because α occurs in a linear term in the equations of motion. The only restriction comes from the property $\phi(\alpha = 0) = 0$ implying the existence of an uniform mode at zero frequency ($U_j = U$ for all j). The precise value of $\tilde{d}$ is given by the slope of $\phi(\alpha)$ near this trivial fixed point. On the gaskets, it is the regularity of the hypertetrahedron that makes the reduction of $\phi(\alpha)$ into a simple quadratic polynomial possible. The degree of this polynomial is fixed by the scaling factor $b = 2$. By a Möbius transformation of the form :

$$\begin{aligned} Z &= -\phi + \delta/2 \\ z &= -\alpha + \delta/2 \end{aligned} \tag{2.13}$$

One obtains the canonical form

$$Z = z^2 - \lambda \tag{2.14}$$

where $\lambda = \delta^2/4 - \delta/2$.

Mappings of the form (2.14) were studied by Julia [12] and Fatou [13], at the beginning of the century and by Brolin [14] very recently. The nature of the spectrum of the gasket and more generally of a self-similar lattice is closely related to the theory of iteration of maps like $\phi(\alpha)$.

3. Functional equation for the Green function and the integrated density of states.

3.1 GENERAL METHOD. — In order to obtain the spectrum of the gasket, we can use the recursion equation 2.8 together with a set of iteration equations for the amplitudes of the eigenstates. Such a method was outlined by Domany *et al.* [15], and will be discussed in section 5 below. However this direct approach requires special boundary conditions in order to be consistent with equation 2.8 at all stages. A more serious limitation of this method comes from difficulties when higher values of d ($d > 3$) are considered, particularly when calculating the eigenmodes and their degeneracy.

The self similarity of the considered structure permits us to write a functional equation for the Green function [16]. The imaginary part of the latter function, and its derivative are closely related to the integrated density of states on the gasket. In the following we shall illustrate the method used for $d = 2$ and $d = 3$ with explicit calculations. The basic trick is this relationship between a symmetrical $n \times n$ matrix A and its determinant :

$$\int_{-\infty}^{\infty} \prod_{i=1}^{n} du_i \exp\left(-\frac{1}{2}\mathbf{u}.A.\mathbf{u} + \mathbf{h}.\mathbf{u}\right) = \left(\frac{(2\pi)^n}{\det A}\right)^{1/2} \exp\left(\frac{1}{2}\mathbf{h}.A^{-1}.\mathbf{h}\right). \tag{3.1}$$

Here $\mathbf{u} = (u_1, ..., u_n)$ denotes a hidden vector, and in our case A represents the dynamical matrix.

Starting with a Gaussian model, on the gasket at stage n :

$$\mathcal{H} = \frac{J}{2} \sum_{\langle ij \rangle} (u_i - u_j)^2 + \mu \frac{J}{2} \sum_i u_i^2 \tag{3.2}$$

its partition function is written (using 3.1) as :

$$Z_n(\mu) = \left(\frac{2\mu}{\beta J}\right)^{N_n/2} G_n(\mu) \tag{3.3}$$

$$= \prod_{i=1}^{N_n} du_i \exp(-\beta\mathcal{H}) \tag{3.4}$$

where $G_n(\mu)$ is given simply by the determinant of the dynamical matrix

$$G_n(\mu) = \prod_{i=1}^{N_n} (\mu + \omega_{i,n}^2)^{-1/2} \tag{3.5}$$

$\{ \omega_{i,n}^2 \}$ are the eigenvalues of the quadratic form (3.2). The integrated density of states is then obtained from the « free energy » per site :

$$\Phi(\mu) = \lim_{n \to \infty} \frac{1}{N_n} \ln G_n(\mu) \tag{3.6}$$

where N_n denotes the total number of sites on the gasket at stage n (Eq. 2.1). If $N(\alpha)$ is used to denote the fraction of modes with squared frequencies below ω^2, one obtains [17] :

$$N(\omega^2) = -\frac{2}{\pi} \operatorname{Im} \Phi(-\omega^2 + i\varepsilon) \tag{3.7}$$

where $i\varepsilon$ is a small imaginary part added to α near the real negative axis. The functional equation is then obtained by first relating G_n to G_{n+1}, and then taking the thermodynamical limit $n = \infty$ (this approach was used for similar problems in Ref. 18).

3.1.1 *Case* $d = 2$. — The relation between G_n and G_{n+1} is obtained using a decimation scheme over all sites at the lowest scale. For instance, consider the terms in $\mathcal{H}$ involving X_1 (see Fig. 1) and its neighbouring sites : $\{ x_i \}$ and $\{ z_i \}$, $i = 1, 2, 3$. This partial Hamiltonian can be decomposed as

$$\hat{\mathcal{H}} = \mathcal{H}_0 + \mathcal{H}_{\text{int}} \tag{3.8}$$

where

$$\mathcal{H}_0 = \frac{\mu J}{2} \sum_{i=1}^{3} (X_i^2 + Z_i^2) \tag{3.9}$$

is a mass term and $\mathcal{H}_{\text{int}}$ contains all other terms in $\hat{\mathcal{H}}$ involving the interactions between sites and mass terms relative to $\{ x_i \}$ and $\{ z_i \}$. The last term can be cast in the form :

$$-\beta\mathcal{H}_{\text{int}} = \left(-\frac{1}{2}\mathbf{u}.G.\mathbf{u} + \mathbf{h}.\mathbf{u}\right) + \left(-\frac{1}{2}\mathbf{v}.G.\mathbf{v} + \mathbf{k}.\mathbf{v}\right) - \beta J \sum_{i=1}^{3} (X_i^2 + Z_i^2) \tag{3.10}$$

where

$$\mathbf{u} = (x_i)_{1 \leqslant i \leqslant 3}, \qquad \mathbf{v} = (z_i)_{1 \leqslant i \leqslant 3}$$

and

$$\begin{aligned} \mathbf{h} &= (X_2 + X_3, X_3 + X_1, X_1 + X_2)\,\beta J \\ \mathbf{k} &= (Z_2 + Z_3, Z_3 + Z_1, Z_1 + Z_2)\,\beta J . \end{aligned} \tag{3.11}$$

In equation 3.10, G is used to denote the 3×3 matrix

$$G_{ij} = \beta J[(\mu + 4)\,\delta_{ij} - (1 - \delta_{ij})] .$$

Performing Gaussian integrations over x_i and z_i, one obtains finally

$$Z_n(J, \mu) = \left[\frac{(2\pi)^3}{\det G}\right]^{-\frac{1}{6}(N_n - N_{n-1})} Z_{n-1}(J', \mu') \quad (3.12)$$

where J' and μ' are the renormalized values of J and μ :

$$J' = J \cdot \frac{\mu + 6}{(\mu + 5)(\mu + 2)} \quad (3.13)$$

$$\mu = \mu(5 + \mu) \quad (3.14)$$

and $\det G = (\beta J)^3 (\mu + 1)^2 (\mu - 2)$ is the determinant of the matrix G.

Using the homogeneity property (λ real)

$$Z_n(\lambda J, \mu) = \lambda^{-N_n/2} Z_n(J, \mu) \quad (3.15)$$

one obtains the desired recursion equation

$$G_n(\mu) = \left[(\mu + 5)^{\frac{N_{n-1} - N_n - N_{n-1}}{2}} \times \right.$$
$$\left. \times (\mu + 2)^{\frac{N_{n-1} - N_n - N_{n-1}}{6}} (\mu + 6)^{-\frac{N_{n-1}}{2}}\right] G_{n-1}(\mu') \quad (3.16)$$

and then the functional equation

$$\Phi(\mu) = \frac{1}{3}\Phi[\mu(\mu + 5)] + \frac{1}{18}\ln\frac{\mu + 2}{(\mu + 5)(\mu + 6)^3} \quad (3.17)$$

3.1.2 *Case* $d = 3$. — Let consider the case $d = 3$ (Fig. 2). As above $\hat{\mathcal{H}}$ is written as (Eq. 3.8), with

$$\mathcal{H}_0 = \frac{\mu J}{2}\left[X_1^2 + \sum_{i=2}^{4}(X_i^2 + Z_i^2)\right] \quad (3.18)$$

and

$$-\beta\mathcal{H}_{\text{int}} = -\frac{3}{2}\beta J\left[2X_1^2 + \sum_{i=2}^{4}(X_i^2 + Z_i^2)\right] +$$
$$+\left(-\frac{1}{2}\mathbf{u}.G.\mathbf{u} + \mathbf{h}.\mathbf{u}\right) + \left(-\frac{1}{2}\mathbf{v}.G.\mathbf{v} + \mathbf{k}.\mathbf{v}\right) \quad (3.19)$$

where

$$\mathbf{u} = (u_2, u_1, u_3, u_4, u_5, u_6)$$
$$\mathbf{v} = (v_2, v_1, v_3, v_4, v_5, v_6) \quad (3.20)$$

and

$$\mathbf{h} = \beta J(X_1 + X_3, X_1 + X_2, X_1 + X_4, X_2 + X_3, X_3 + X_4, X_2 + X_4) \quad (3.21)$$

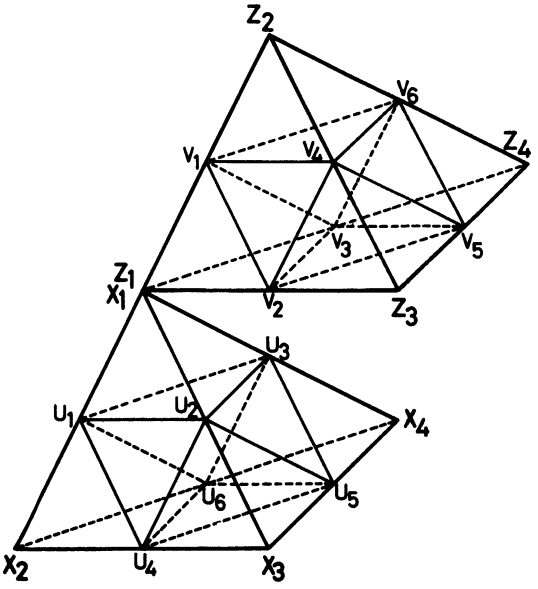

Fig. 2. — Part of a 3-dimensional Sierpinski gasket, at the lowest scale.

$$\mathbf{k} = \beta J(Z_1 + Z_3, Z_1 + Z_2, Z_1 + Z_4, Z_2 + Z_3, Z_3 + Z_4, Z_2 + Z_4)$$

The 6×6 matrix G is given by

$$G_{ij} = \beta J[(\mu + 6)\delta_{ij} - (1 - \delta_{i+j,7})], \quad 1 \leqslant i, j \leqslant 6 \quad (3.22)$$

with a determinant

$$\det G = (\beta J)^6 (\mu + 6)^3 (\mu + 3)^2 (\mu + 2). \quad (3.23)$$

Using the same decimation procedure as for $d = 2$, one obtains

$$\mu' = \mu(\mu + 6) \quad (3.24)$$

$$J' = J\frac{\mu + 8}{(\mu + 6)(\mu + 2)} \quad (3.25)$$

and

$$G_n(\mu)/G_{n-1}(\mu') = (\mu + 6)^{\frac{N_{n-1} - N_n - N_{n-1}}{4}} \times$$
$$\times (\mu + 8)^{-\frac{N_{n-1}}{2} - \frac{N_n - N_{n-1}}{6}} \cdot (\mu + 2)^{\frac{N_{n-1} - N_n - N_{n-1}}{12}} \quad (3.26)$$

From the last recursion equation, it is easy to deduce the following functional equation for $\Phi(\mu)$:

$$\Phi(\mu) = \frac{1}{4}\Phi[\mu(\mu + 6)] + \frac{1}{16}\ln\frac{\mu + 2}{(\mu + 6)(\mu + 8)^4} \quad (3.27)$$

which is analogous of the equation (3.17) for the case $d = 3$.

3.1.3 *Case of general d.* — A straightforward generalization of the above decimation procedure yields, for general d, the following results :

$$\mu' = (\mu + d + 3) \tag{3.28}$$

$$J' = J \cdot \frac{\mu + 2d + 2}{(\mu + d + 3)(\mu + 2)} \tag{3.29}$$

and

$$\Phi(\mu) = \frac{1}{(d+1)} \Phi[\mu(\mu + d + 3)] + \\ + \frac{d-1}{2(d+1)^2} \ln \frac{\mu + 2}{(\mu + d + 3)(\mu + 2d + 2)^{d+1}} \cdot \tag{3.30}$$

The coefficient in front of the last term in equation 3.30 is given by

$$\lim_{n \to \infty} \frac{1}{N_n} \left[\frac{1}{2} N_{n-1} - \frac{N_n - N_{n-1}}{2\binom{d+1}{2}} \right] = \frac{d-1}{2(d+1)^2} \tag{3.31}$$

As it should be, we recover the equations 3.17 and 3.27 for $d = 2$ and $d = 3$ respectively. For $d = 1$, a direct calculation leads to equations 3.28-30. In this particular case one observes the absence of the second term in the right side of equation 3.30. The occurrence of this term at $d > 1$ is at the origin of a qualitative change in the nature of the spectrum when compared to that at $d = 1$.

It should also be noted that the map ϕ, given by equation 2.8, appears in the argument of the function Φ on the right-side of equation 3.30. Such behaviour is naturally associated with the self-similarity of the gasket, expressing the general relationship between functional equations and map iteration theories [19]. The functional equation 3.30 for Φ contains all the information about the spectrum of the gasket and is used in the following for the calculation of the integrated density of states. Besides the trivial case $d = 1$, where equation 3.30 reduces to the well-known Schröder-Abel equation [19, 20], we have no systematic procedure to solve equation 3.30. Additional conditions (continuity, differentiability, ...) are needed to find non trivial solutions for this equation. For detailed studies of functional equations in a single variable, we direct the reader to the classical monographs [Refs 10 and 20].

3.2 THE INTEGRATED DENSITY OF STATES. — In spite of the difficulties involved in finding a general solution for equation 3.30, general features of the spectrum can be extracted from this functional equation. For instance, for $\mu \gg 1$, equation 3.30 reduces to

$$\Phi(\mu) \simeq \frac{1}{d+1} \Phi(\mu^2) + \frac{d-1}{2(d+1)^2} \ln \mu^{-(d-2)} \tag{3.32}$$

which has a solution given by

$$\Phi(\mu) = -\frac{1}{2} \ln \mu . \tag{3.33}$$

Starting with this limiting solution, we can obtain an analytical continuation for $\Phi(\mu)$ defining this function in the whole μ complex plane and taking real values on the positive real axis. Branch cuts are used on the negative real axis because of the occurrence of logarithmic branching points produced by the right term in equation 3.30. When the negative real axis ($\mu < 0$) is crossed the values of $\Phi(\mu)$ differ by an imaginary constant. Taking the imaginary part of equation 3.30 close to the negative real axis, and using equation 3.7, we deduce the following relations for the integrated density of states

$$N(\alpha) = \frac{1}{d+1} N[\phi(\alpha)] - \frac{d-1}{(d+1)^2} \theta(\alpha - 2), \quad \text{for} \quad 0 < \alpha < \frac{d+3}{2} \tag{3.34}$$

$$N(\alpha) = -\frac{d-1}{(d+1)} \{ \theta(\alpha - 2) - \theta(\alpha - d - 3) - (d+1)\, \theta(\alpha - 2d - 2) \} + \frac{2}{d+1} - \frac{1}{d+1} N[\phi(\alpha)]$$

$$\text{for} \quad \frac{d+3}{2} < \alpha < \infty$$

where $\theta(x)$ denotes the step function ($\theta(x) = 1$ for $x > 0$ and $\theta(x) = 0$ for $x < 0$). The integrated density of states is therefore completely determined, using the functional relations 3.34. We found that $N(\alpha)$ is a constant function almost everywhere on the real axis (see below), and a monotonically increasing function of α. The spectrum is confined in the interval $[0, 2d + 2]$, with

$$N(\alpha) = 0 \quad \text{for} \quad \alpha \leqslant 0 \\ N(\alpha) = 1 \quad \text{for} \quad \alpha \geqslant 2d + 2 \tag{3.35}$$

Using equations 3.34-3.35, the obtained integrated density of states is a highly singular function of α, giving rise to a nontrivial spectrum for the gasket.

4. Spectrum and eigenmodes.

The iteration scheme suggested by the equations 3.34-3.35 is used in this section in order to find $N(\alpha)$ on the whole real axis. In the following we shall illustrate briefly this procedure, as well as the calculation of the eigenmodes associated with the spectrum.

4.1 NATURE OF THE SPECTRUM. — The function $N(\alpha)$ is known (Eq. 3.35) outside the interval $[0, 2(d + 1)]$ containing the spectrum of the gasket. Repeated applications of equation 3.34 involve the map $\phi(\alpha)$ and its inverse

$$f_{\pm}(\alpha) = \tfrac{1}{2}[\delta \pm \sqrt{\delta^2 - 4\alpha}]. \qquad (4.1)$$

The qualitative features of the spectrum are very sensitive to the relative value of the « control parameter » $\delta = d + 3$ in respect to the « critical » value $\delta_c = 4$, corresponding to the linear chain ($d = 1$). In the following we limit ourselves to the case $\delta > \delta_c$. The case of the harmonic linear chain is discussed separately at the end of this section. In general, the spectrum of the gasket is the superposition of two distinct parts : a pure point spectral measure of relative weight $d/(d + 1)$, supported by a set of Lebesgue measure zero; and a second pure point spectral measure of relative weight $1/(d + 1)$, supported by a Cantor set of Lebesgue measure zero.

4.1.1 *First part of the spectrum.* — The graph of the map $\phi(\alpha)$ is sketched in figure 3. The two unstable fixed points are located at $\alpha = 0$ and $d + 2$, $\phi(\alpha)$ reaches its maximum value at $\alpha_m = \delta/2$ where $\phi(\alpha_m) = \delta^2/4$. The upper edge of the spectrum has two predecessors : $\alpha = 2$ and $\alpha = d + 1$. Using equations 3.34 and 3.35, we obtain

$$N(\alpha) = \frac{2}{(d + 1)} \quad \text{for} \quad d + 3 < \alpha < 2(d + 1). \qquad (4.2)$$

A first jump occurs therefore at the upper edge of the spectrum. The height of this jump is given by

$$\Delta' = (d - 1)/(d + 1). \qquad (4.3)$$

A second use of equation 3.34 permits us to obtain the function $N(\alpha)$ in a new α-interval :

$$N(\alpha) = 2/(d + 2)^2 \quad \text{for} \quad \alpha_1 < \alpha < d + 1$$
$$= 1/(d + 1) \quad \text{for} \quad d + 1 < \alpha < \alpha_2 \qquad (4.4)$$

where α_1 and α_2 ($> \alpha_1$) are solutions of the equation $\phi(\alpha) = d + 3$. A new jump of the function $N(\alpha)$ of height $\Delta_0 = (d - 1)/(d + 1)^2$ is then obtained at $\alpha = d + 1$. Repeated applications of $f_{\pm}$ give the successive images of the basic « cell » shown in figure 4. At each stage of the iteration, every jump of height Δ_i gives rise to two jumps, of equal heights : $\Delta_{i+1} = \Delta_i/(d + 1)$. Such a procedure generates therefore a pure point spectral measure (discrete spectrum) supported by a set of Lebesgue measure zero. The eigenfrequencies are located at $\alpha = 2d + 2$ and at $\alpha = d + 1$ and its successive images by $f_{\pm}$. This part of the spectrum of the gasket is self-similar by construction; its relative weight is given by the sum ($d > 1$) :

$$\Delta' + \sum_{i=0}^{\infty} 2^i \Delta_i = d/(d + 1). \qquad (4.5)$$

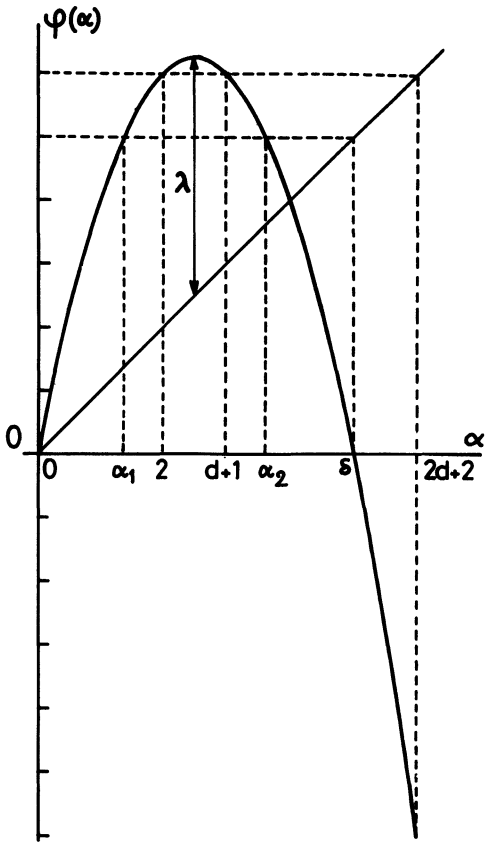

Fig. 3. — The graph of the map $\phi(\alpha) = \delta\alpha - \alpha^2$, for a d-dimensional structure, where $\delta = d + 3$ and $\lambda = \delta^2/4 - \delta/2$. α_1 and α_2 are the two solutions of the equation $\phi(\alpha) = \delta$.

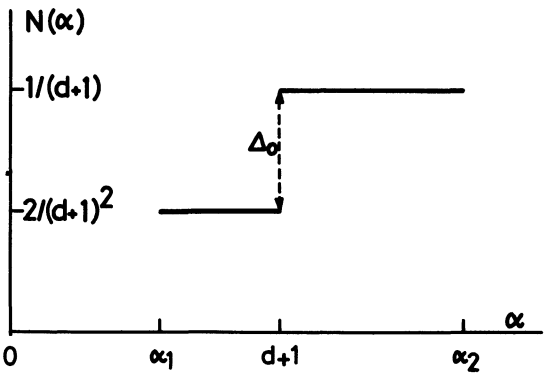

Fig. 4. — Elementary cell in the iteration $f_{\pm}(\alpha)$ (see text), showing the occurrence of the jump Δ_0 at $\alpha = d + 1$, after the first iteration.

To each jump of $N(\alpha)$ is associated naturally a highly degenerate eigenmode (see Fig. 5).

4.1.2 *Second part of the spectrum.* — The second part of the spectrum, of relative weight $1/(d+1)$, is given by the Julia [14] set associated with the map ϕ (i.e. the complementary set of the attraction domain of the fixed point at infinity $\alpha = \infty$). This part of the spectral measure is associated with a Cantor spectrum, supported by a compact perfect set C_δ : the Cantor set of Lebesgue measure zero, given by

$$\{ C_\delta \} = \left\{ \frac{\delta}{2} + \sigma_0 \sqrt{\lambda + \sigma_1 \sqrt{\lambda + \sigma_2 \sqrt{\lambda + \cdots \text{ (ad infinitum)}}}} \right\} \tag{4.6}$$

where $\lambda = \delta^2/4 - \delta/2$ and $\sigma_i = \pm 1$.

This set is obtained, as above, by repeated applications of equation 3.34. After the first iteration, the function $N(\alpha)$ is calculated in the interval $\left]\frac{\delta}{2} - \sqrt{\lambda - \frac{\delta}{2}}, \frac{\delta}{2} + \sqrt{\lambda - \frac{\delta}{2}}\right[$ which can be removed. At the second stage, one obtain a support contained in the set

$$\left]\frac{\delta}{2} - \sqrt{\lambda + \sqrt{\lambda - \frac{\delta}{2}}}, \frac{\delta}{2} - \sqrt{\lambda - \sqrt{\lambda - \frac{\delta}{2}}}\right[\cup \left]\frac{\delta}{2} + \sqrt{\lambda - \sqrt{\lambda - \frac{\delta}{2}}}, \frac{\delta}{2} + \sqrt{\lambda + \sqrt{\lambda - \frac{\delta}{2}}}\right[. \tag{4.7}$$

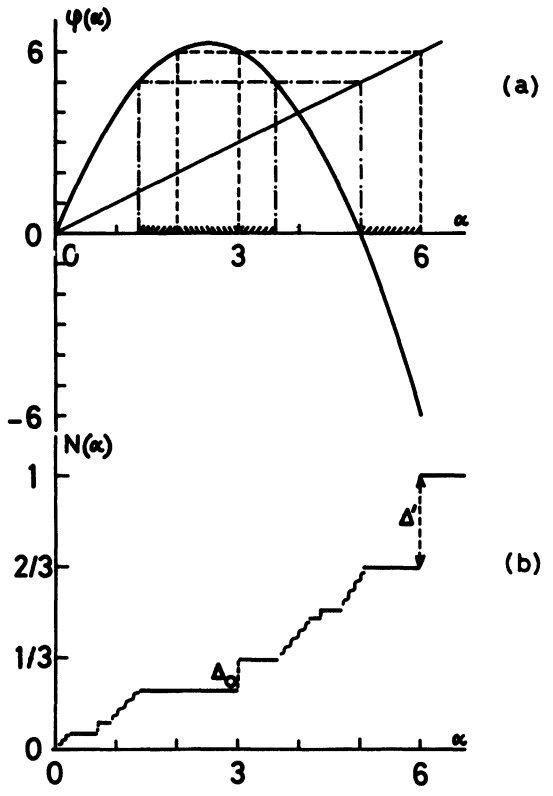

Fig. 5. — *a*) Successive steps in the application of $f_\pm(\alpha)$, at $d = 2$. *b*) Behaviour of the integrated density of states $N(\alpha)$, at $d = 2$, after the first iterations. The jumps of heights Δ' and Δ_0 correspond to eigenfrequencies in the first part of the spectrum.

At each stage n, one obtains a support which consists of 2^{n-1} such intervals. When $n \to \infty$ the gaps tend to be dense and therefore the second part of the spectral measure is supported by the Cantor set C_δ given by equation 4.6. This construction gives finally the graph of $N(\alpha)$ shown on figure 5. The resulting function $N(\alpha)$ is a continuous bounded monotonic non decreasing function whose derivative exists and is zero at every point except on the support of the spectral measure.

Each eigenfrequency given by (4.6) is naturally coded by an infinite sequence $\{ \sigma \}$, where $\sigma_i = \pm 1$. For instance, the sequence $\sigma_i = +1$ corresponds to $\alpha = d + 3$, and that with $\sigma_i = -1$ corresponds to $\alpha = 0$. Therefore (4.6) can be generated by repeated applications of $f_\pm$ starting from $\alpha = 0$. Successive jumps for $N(\alpha)$ are also generated as above : Δ_0 at $\alpha = d + 3, \ldots$ and the total weight is given by :

$$\sum_{i=0}^{\infty} 2^i \Delta_i = 1/(d+1) . \tag{4.8}$$

The above coding (4.6) of the Cantor spectrum permits to show the invariance of this spectrum under ϕ and $f_\pm$ [21, 22] :

$$\phi(\alpha \{ \sigma \}) = \alpha(T \{ \sigma \}) \tag{4.9}$$

$$f_\pm(\alpha \{ \sigma \}) = \alpha(\pm, \{ \sigma \}) \tag{4.10}$$

where T denotes the « shift » operator

$$T(\{ \sigma_0, \sigma_1, \ldots \}) = \{ -\sigma_1, \sigma_2, \ldots \} \tag{4.11}$$

and

$$(\pm, \{ \sigma \}) = \{ \pm, -\sigma_0, \sigma_1, \ldots \} . \tag{4.12}$$

To our knowledge, this kind of spectrum was first encountered in physical problems by Bellissard *et al.* [21] in their work on the socalled « quadratic mapping Hamiltonian ». These authors have studied a one dimensional crystallographic model, associated with an almost periodic potential, and assuming a spectrum similar to (4.6). The main difference between the two cases is the nature of the spectral measure

The absence of an atomic part in the spectral measure of the quadratic mapping Hamiltonian leads to a singular continuous spectral measure. In the case of the gasket, the spectrum is given by (4.6) but the associated spectral measure is a pure point one. This difference comes from the relative weight of the sequences $\{ \sigma \}$ in (4.6) which is the same in the first case and not in the second case. Otherwise, the second part of the gasket's spectral measure is made of Dirac functions sitting on a denumerable subset of the Julia set. Only its closure coincides with the Julia set which contains a non denumerable set of points. (This subtle difference is of great importance from measure theory viewpoint, but will not be discussed further here.)

4.2 EIGENMODES ($d > 1$). — The iterative scheme used in the above section can also be used to find the eigenmodes on the gasket. Having an eigenmode associated with α, we can obtain using the maps ϕ and $f_{\pm}$ the set of eigenmodes corresponding to other eigen-frequencies. Two kinds of states are obtained : localized « molecular » states associated with the first part of the spectrum, and hierarchical localized states associated with the Cantor spectrum. To be clear, the discussion below is limited to the case $d = 2$. All obtained results hold also for any $d > 1$.

4.2.1 *Localized « molecular » modes.* — We start by calculating the eigenmodes associated with the upper edge of the spectrum $\alpha = 2(d + 1)$. The corresponding amplitudes are easily obtained from the equations of motion. These modes are degenerate, exhibiting clearly the rotation invariance of the gasket. For instance, at this frequency $\alpha = 6$, there are three eigenmodes (Fig. 6), ψ_1, ψ_2 and ψ_3 localized inside each triangle of side 4 a (a denotes the length of the lowest scale side on the gasket). These $N_n/3$ modes are similar to the well-known band edge modes in crystals, as can be seen in figure 7*a*, where $(\psi_1 + \psi_2 + \psi_3)$ is shown. The main property of these localized modes is the vanishing of the amplitude U_n's, outside a finite set of sites. This behaviour holds also for the other frequencies of the first part of the spectrum. For instance, at $\alpha = \phi^{-1}(6) = 3$ the corresponding mode is shown on figure 7*b*. Because of this peculiarity, we call these modes : « molecular » eigenmodes.

In order to quantify these more than localized states, we use their extension range $L(\alpha)$, such that $L^{\bar{d}}(\alpha)$ measures the occupation « volume » of the mode associated with α. For instance, $L(\alpha = 6) = 2\,a$, $L(\alpha = 3) = 4\,a$. It is clear, for $n \geqslant 1$, that L is given by

$$L(\phi^{-n}(\alpha = 6)) \simeq 2^{n+1}\, a\,. \qquad (4.13)$$

At low frequencies, $L(\alpha)$ is given by

$$L/a \simeq (\omega_0/\omega)^k \qquad (4.14)$$

where k is an exponent given by

$$k = 2 \ln 2/\ln 5 = \tilde{d}/\bar{d}\,. \qquad (4.15)$$

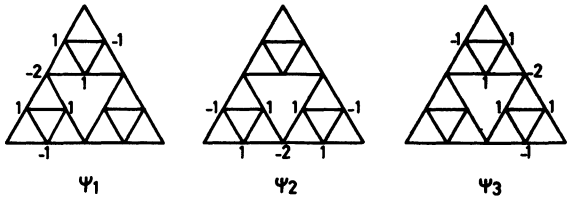

Fig. 6. — Eigenstates associated with the upper edge of the spectrum ($\alpha = 6$) at $d = 2$. Only non vanishing amptitudes are shown of the figure.

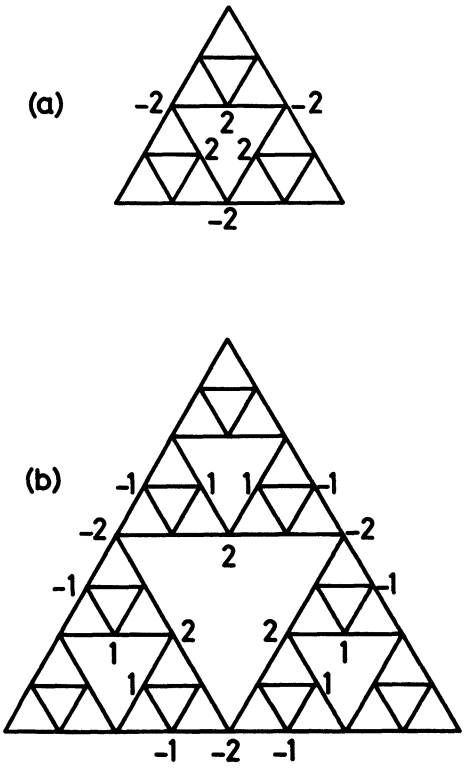

Fig. 7. — *a*) The eigenmode $\psi = (\psi_1 + \psi_2 + \psi_3)$ associated with $\alpha = 6$ (see Fig. 6). *b*) The eigenmode associated with $\alpha = 3 = \phi^{-1}$ (6), deduced from ψ. As in figure 6, only non vanishing amptitudes are shown.

The divergence of the range $L(\alpha)$ at $\omega \to 0$ is naturally associated with the accumulation point $\alpha = 0$ corresponding to the uniform extended mode. The result (4.15) can be obtained directly with the help of the following scaling argument. For a given α in the spectrum, $L(\alpha)$ must be a solution of the scaling equation ($b = 2$) :

$$L(\phi(\alpha)) = \frac{1}{2}\, L(\alpha) \qquad (4.16)$$

In particular, if $L(\alpha)$ diverges at $\omega \to 0$, with an exponent k, equation 4.16 gives immediately the value of this exponent as

$$k = 2.\ln 2/|\ln \phi'(0)| = \tilde{d}/\bar{d}. \qquad (4.17)$$

The « localization » volume scales therefore like $(L(\omega))^{\bar{d}} \simeq \omega^{-\bar{d}}$. For each eigenfrequency α, the corresponding degenerate eigenstates obtained above are independent, but they are not orthogonal. A straightforward orthogonalization procedure can be outlined within each degenerate subspace.

4.2.2 « *Hierarchical* » *modes.* — We now turn to calculate the eigenmodes associated with the Cantor spectrum (4.6). The starting point here is the lowest edge of the spectrum $\alpha = 0$ corresponding to the uniform mode, from which we deduce the amplitudes corresponding to $\alpha = d + 3 = \phi^{-1}(0)$. To this value of α is associated a degenerate mode localized around the holes inside the gasket. The corresponding amplitudes are non zero only inside a triangle surrounding the chosen hole and the relative degeneracy, for a given $\alpha \in C_\delta$, decreases when the hole size increases. Therefore to each $\alpha \in C_\delta$ is associated a hierarchy of localization lengths standing from a finite value $L_1(\alpha)$ to $L_2(\alpha) = \infty$, and corresponding to the increasing size of holes. For this reason, we call these modes « hierarchical » modes. However these degenerate states do not mix to create extended states. In particular, if an « averaged » localization length is defined for each $\alpha \in C_\delta$, then a finite length is obtained $\bar{L}(\alpha)$, which is a solution of equation 4.16. As above $\bar{L}(\alpha)$ diverges at $\alpha \to 0$ with the exponent $k = \tilde{d}/\bar{d}$.

4.2.3 *General features of the eigenmodes.* — In general the eigenmodes can be expressed with the family of orthogonal polynomials $\{ P_n \}$ introduced in reference 22. $\{ P_n \}$ fulfills a three-term recursion relation

$$P_{n+1} = -(\alpha - \delta/2) P_n - R_n P_{n-1} \qquad (4.18)$$
$$P_{-1} = 0, \quad P_0 = 1, \quad P_1 = -\alpha + \delta/2$$

where R_m's are rational fraction in $\lambda = \delta^2/4 - \delta/2$, generated by the recursion relation

$$R_0 = 0, \quad R_1 = \lambda, \quad R_{2m} R_{2m-1} = R_m, \quad R_{2m} + R_{2m+1} = \lambda. \qquad (4.19)$$

Besides trivial properties (degree, parity, ...) of the family $\{ P_n \}$, we have the important property : for any positive integer n, we have

$$P_{2n}(\alpha) = P_n(\phi(\alpha)) \qquad (4.20)$$

and more generally

$$P_{n.2^k}(\alpha) = P_n(\phi^{(k)}(\alpha)), \quad k \text{ integer} \qquad (4.21)$$

where $\phi^{(k)}$ is the k-th iterate of the map ϕ.

The set of polynomials $\{ P_n \}$ is appropriate for the dilation symmetry of the gasket : equation 4.21 exhibits clearly this property. From this view point $\{ P_n \}$'s are therefore the counterpart of the Bloch waves in translation invariant structure. In the particular case $d = 1$, $\{ P_n \}$ reduces the well-known Tchebychev polynomials $\{ T_n \}$, where dilation and translation symmetries coexist (see section 4.3).

The general pattern of the amplitudes corresponding to a given α is illustrated on figure 8. If we choose the site ω as the origin, and label the sites along the external edge of the gasket by the integers n, one obtains the scaling relation :

$$U_{n.2^k}(\alpha) = U_n(\phi^{(k)}(\alpha)). \qquad (4.22)$$

For $\alpha \in C_\delta$, (4.22) can also be written as

$$U_{n.2^k}(\alpha) = U_n(\alpha(T^k(\{ \sigma \}))) \qquad (4.23)$$

which is a direct consequence of the invariance of C_δ under ϕ. Exceptional sequences $\{ \sigma \}$ can be periodic, leading to a periodic behaviour of $k \to U_{n.2^k}$, but this happens with probability zero. An example of this kind of periodic mode is shown in figure 9*a* and corresponds to the fixed point $\alpha = 4$ obtained for the sequence $\{ \sigma \}$: $\sigma_0 = 1$, $\sigma_1 = -1$ and $\sigma_i = 1$ $(i \geqslant 2)$. An example of hierarchical states corresponding to $\alpha = 5$ is also shown in figure 9*b*. In general, no simple rule was obtained between U in (4.22) and P in (4.20).

4.3 Case $d = 1$. — When $\delta = \delta_c = 4$, the functional equation for $\Phi(\mu)$ reduces to

$$\Phi(\mu) = \tfrac{1}{2} \phi[\mu(\mu + 4)] \qquad (4.24)$$

and the integrated density of states $N(\alpha)$ becomes the solution of the equation

$$N(\alpha) = \tfrac{1}{2} N[\phi(\alpha)], \quad 0 < \alpha < 2$$
$$= \tfrac{1}{2} - \tfrac{1}{2} N[\phi(\alpha)], \quad 2 < \alpha < 4 \qquad (4.25)$$

obeying the boundary conditions

$$N(\alpha < 0) = 0, \quad N(\alpha \geqslant 4) = 1. \qquad (4.26)$$

The function $N(\alpha)$ verifies also the duality relation

$$N(\alpha) + N(4 - \alpha) = 1. \qquad (4.27)$$

We found (Fig. 10*b*) :

$$N(\alpha) = \frac{1}{\pi} \text{Arc sin} \left(\frac{\alpha}{4}\right)^{1/2} \qquad (4.28)$$

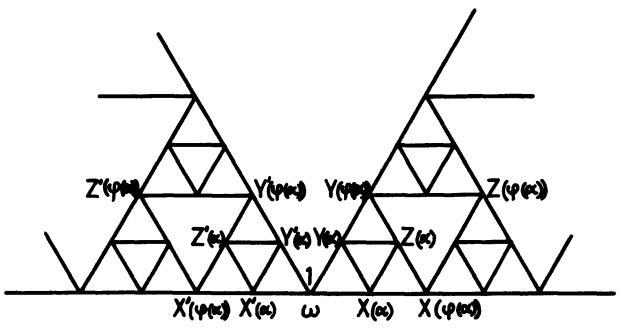

Fig. 8. — Different amptitudes on an infinite gasket. The site denoted ω was chosen as origin.

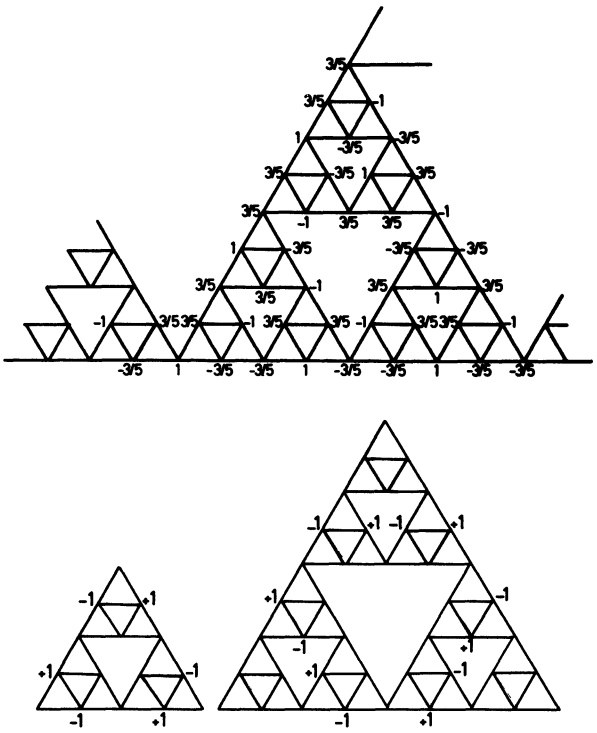

Fig. 9. — Example of : *a*) periodic state associated with the eigenvalue $\alpha = 4$, *b*) hierarchical state associated with the eigenvalue $\alpha = 5$ for the gasket at $d = 2$.

recovering then the known power law

$$N(\alpha) \sim \alpha^{1/2} \quad \text{at} \quad \alpha \sim 0 . \tag{4.29}$$

The procedure outlined above for the case $\delta > \delta_c$ continues to work in the critical case. For this critical value of δ, ϕ maps the interval [0, 4] exactly into itself (Fig. 10*a*), and the first part of the spectrum obtained at $\delta > 4$ disappears. Only the Cantor spectrum $C_{\delta=4}$ remains, becoming a dense set in the interval [0, 4]. In fact [23], every real number $\alpha \in [0, 4]$ can be written as ($\lambda = 2$) :

$$\alpha = 2 + \sigma_0 \sqrt{2 + \sigma_1 \sqrt{2 + \sigma_2 \sqrt{2 + \cdots}}} \tag{4.30}$$

where $\sigma_i = \pm 1$.

In the limiting case $\delta = \delta_c$ all the gaps in the spectrum support [0, 4] become filled up and the resulting measure is absolutely continuous. The sequence $\{ R_n \}$ defined by equation 4.19 becomes ($\lambda = 2$) :

$$R_0 = 0 , \quad R_1 = 2 \quad \text{and} \quad R_n = 1 \qquad (n > 2) . \tag{4.31}$$

The family of polynomials $\{ P_n \}$ reduces to that of Tcheybychev polynomials $\{ T_n \}$ obeying the recursion relation

$$T_{n+1}(x) = 2 x T_n - T_{n-1} \tag{4.32}$$

with

$$T_0 = 1 , \quad T_{\pm 1} = x .$$

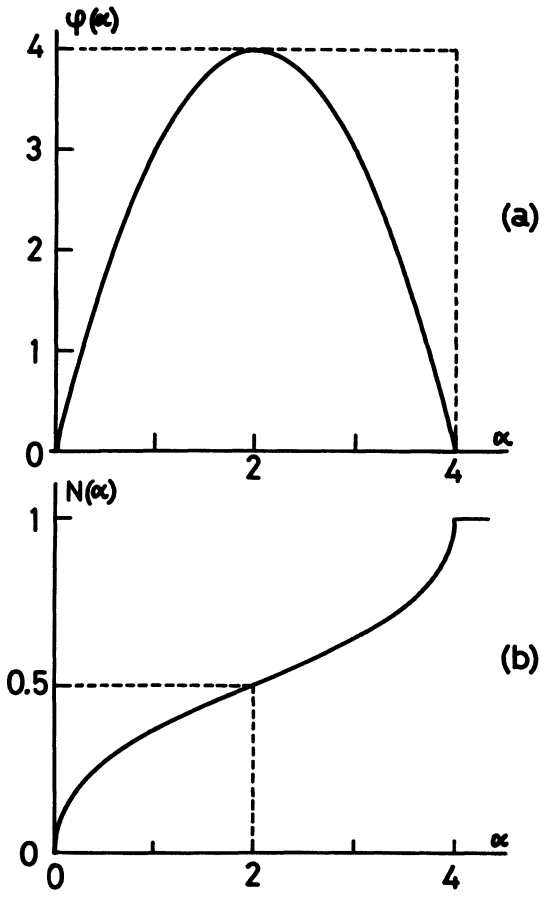

Fig. 10. — *a*) The graph of the map $\phi(\alpha) = 4\alpha - \alpha^2$ at $d = 1$. *b*) The integrated density of states $N(\alpha)$ as function of α, for the same value of d.

When the variable x in the argument of T_n's is identified with the reduced variable $x = (2 - \alpha)/2$, one obtains for even modes ($U_0 = 1$, $U_{-n} = U_n$) the following solution

$$U_n(\alpha) = T_n(x = 1 - \alpha/2) . \tag{4.33}$$

Using the well-known relation, $T_n(\cos\theta) = \cos n\theta$, we recover :

$$U_n(\alpha) = T_n(\cos\theta) = \cos n\theta \tag{4.34}$$

which is nothing else than the known Bloch wave, appropriate for the translation symmetry of the linear chain. In addition it is easy the verify the scaling property

$$U_{n.2^k}(\alpha) = U_n(\phi^{(k)}(\alpha)) \tag{4.35}$$

exhibiting the dilation symmetry of the chain.

The limiting case of the linear chain shows therefore the connection between two different symmetries : dilation and translation which coexist together in this case. It is interesting to remark the occurrence of a chaotic behaviour associated with the map $\phi(\alpha) = 4\alpha - \alpha^2$, but without any effect on standard physical properties such as the spectrum of the chain.

To summarize, the spectrum of the Sierpinski gasket is very sensitive to the relative value of the « control parameter », δ. For $\delta > 4$ (i.e. $d > 1$) the spectral measure is the superposition of two distinct parts, given by two pure point spectral measures of relative weights $d/(d+1)$ and $1/(d+1)$ respectively. At $\delta = \delta_c$, the spectral measure degenerate into an absolutely continuous one, supported by a band spectrum [0, 4].

Evidently the model loses its meaning at $d < 1$, but in this sector $0 < \delta < 4$ the function $\phi(\alpha)$, when restricted to the domain $[0, \delta]$, maps this interval into itself. Phenomena like double-period bifurcation, occurrence of chaos bands, etc., are known to occur precisely in this sector. The limiting value $\delta = \delta_c$ can then be viewed as a critical point for the one parameter family of maps $\phi_\delta(\alpha)$. The qualitative change at $\delta = \delta_c$ is closely related to the topological features of the Julia set, associated with this map, as a function of the parameter δ.

5. Influence of the boundary conditions. Comparaison with other works.

In the preceding section, we have used an iteration scheme, mainly based on the validity of equation 2.8. Such an assumption is only correct on an infinite gasket, or for periodic boundary conditions (Ref. 15). In this section, we shall investigate the influence of the boundary conditions on the spectrum of the gasket. We also compare our results with those obtained by other authors.

5.1 Finite gaskets.

5.1.1 *Free boundary conditions.* — It is sufficient to consider the case $d = 2$. Let consider the Sierpinski gasket of order n, obtained as explained in section 2. Using the decimation scheme outlined in section 2, we reduce the search of the spectrum to that at stage $n = 0$ (simple triangle). However, the free boundary conditions introduce a further complication, because the three external sites are not equivalent to internal sites and equation 2.8 breaks down for these sites. Two parameters are involved in the decimation procedure : $\alpha = m\omega^2/K$ for internal sites and $\alpha' = m'\omega^2/K$ for three external sites. The iteration equations are written :

$$\alpha_{i+1} = \alpha_i(5 - \alpha_i)$$
$$\alpha'_{i+1} = \frac{4(5-\alpha_i)}{6-\alpha_i} + (\alpha'_i - 2)\frac{(2-\alpha_i)(5-\alpha_i)}{6-\alpha_i} \qquad (5.1)$$

with the starting point

$$\alpha_0 = \alpha'_0 = m\omega^2/K . \qquad (5.2)$$

The N_n eigenfrequencies are then given by

$$\alpha'_n = 0 \quad \text{(simple)}$$
$$\alpha'_n = 3 \quad \text{(doubly degenerate)} \qquad (5.3)$$

with the exclusion rule $\alpha_{n-1} \neq 5$ and $\alpha_{n-1} \neq 2$.

Equation 5.3 can also be written as follows :

$$\alpha'_{n-1} = \frac{2\alpha_n - 1}{\alpha_{n-1} - 2} \quad \text{(simple)} \qquad (5.4)$$

and

$$\alpha'_{n-1} = \frac{2\alpha_{n-1} - 9}{\alpha_{n-1} - 5} \quad \text{(doubly degenerate)} .$$

At low frequencies ($\alpha_0 \ll 5^{-n-1}$), equation 5.1 yields

$$\alpha_n \simeq 5^n \alpha_0 , \quad \alpha'_n \simeq \tfrac{1}{2} 5^n \alpha_0 \qquad (5.5)$$

showing clearly the influence of the free boundary conditions. In terms of masses, equation 5.5 can be written as

$$m_n \simeq 5^n . m , \quad m'_n \simeq \tfrac{1}{2} m_n . \qquad (5.6)$$

Using equation 5.4, we have calculated the spectral density for $n = 0$, 1 and 2 (see Fig. 11) : almost all eigenfrequencies are degenerate.

The nature of the associated eigenmodes depends on the relative position of α_i's with respect to the Julia set (see section 4). For instance, if α_i does not belong to the Julia set for every $i \leqslant n$, then for $n \gg 1$, $|\alpha_i|$ becomes bigger and bigger and $\alpha_i \to \infty$. For such eigenvalues, the gasket breaks into smaller triangles, and the eigenstates are localized on these triangles, decaying exponentially outside. This part of the spectrum is expected to evolve and then « converges » towards the first part found in section 4.

For eigenfrequencies α, such that there exists α_n ($k < n$) belonging to the Julia set, the amplitudes

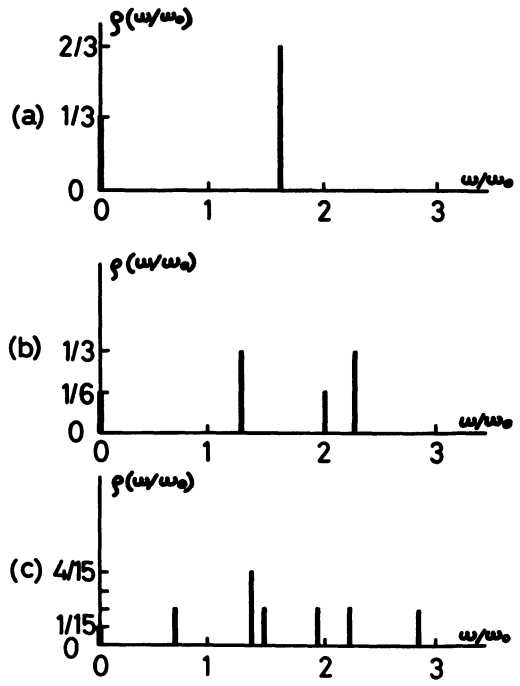

Fig. 11. — Spectral density $\rho(\omega/\omega_0)$ for the finite gaskets (with free boundary conditions) as function of the reduced frequency ω/ω_0. *a*) $n = 0$, *b*) $n = 1$, *c*) $n = 2$.

of the eigenmodes become localized inside triangles of side l^* ranging from the lowest to the highest length scale $2^k a \lesssim l^* \leqslant 2^n a$. These values of α are expected to generate the Cantor spectrum obtained in section 4, which appears only at $n = \infty$.

5.1.2 *Periodic boundary conditions.* — This type of boundary conditions (Ref. 15) is more appropriate to describe the asymptotic approach ($n = \infty$), because equation 28 is preserved everywhere. The idea is to use a « replicated » gasket obtained by the juxtaposition of two identical n stage gaskets at their corresponding external sites. A direct calculation of the spectrum for $d = 2$ is outlined in reference 15, and the main conclusions fully agree with ours.

5.2 COMPARISON WITH OTHER WORKS. — The distribution of modes in vibrating fractal system was recently considered from another viewpoint by Berry [24]. He considered a region R of d-dimensional space with boundary ∂R which is d'-dimensional ($d' = d-1$ for Euclidean space), and the eigenvalue (resonator problem)

$$(\nabla^2 + k_n^2)\,\psi_n = 0 \quad \text{in} \quad R \tag{5.7}$$

$$\psi_n = 0 \quad \text{on} \quad \partial R \tag{5.8}$$

where ψ_n is an eigenfunction associated with the eigenvalue k_n. If M_d (resp. $M_{d'}$) is the measure of R (resp. ∂R) then it is known [25, 26] that the asymptotic mode number $N(k)$, defined as the number of modes with $k_n < k$ (at $k \to 0$), is given by the Weyl-Kac formula

$$N(k) = \frac{M_d}{(d/2)\,!\,(4\pi)^{d/2}}\,k^d - \frac{M_{d'}}{4(d'/2)\,!\,(4\pi)^{d'/2}}\,k^{d'} + \cdots \tag{5.9}$$

Berry has conjectured that equation 5.9 remains valid when R and/or ∂R are fractals provided d and d' are interpreted as fractal dimensions and M_d and $M_{d'}$ are the fractal measures of R and ∂R. The above formula was justified on scaling ground arguments and a « smoothing » procedure. However, as pointed out by Berry, ∇^2 cannot be expressed in d-dimensional coordinates. By using a discrete approximation of ∇^2 on a grid, sampling R on the scale $\lambda = 2\pi/k$ of the wave length, we recover a set of finite difference equations like equation 2.5. The above study shows the occurrence of a new number $\tilde{d}$ in the expression of $N(\omega^2)$ instead of $\bar{d}$ as claimed by Berry. The difficulties with equation 5.9 lie at the following level. Formally one can define some local geometry on the fractal, in which the Laplacian has its usual form, i.e. equivalent to a local k^2-expansion. However, the mode counting in reciprocal space is described by the spectral dimensionality $\tilde{d}$, which is relevant for a standard Laplacian expansion. $\tilde{d}$ determines a natural expansion of a gradient expansion to fractals. An alternative of expanding in Euclidean gradients leads to an expansion in $k^{2\bar{d}/\tilde{d}}$ instead of in k^2, and then a reciprocal space of dimensionality $\bar{d}$. For these reasons, equation 5.9 is doubtful when used for fractal structures.

6. Conclusion.

We believe that the results obtained in this paper are general and that similar features will be found to occur on other fractal structures. The map $\alpha \to \phi(\alpha)$ is expected to be a general rational function. It will also be quite useful to study other fractal structures as simple as the gasket where $\tilde{d}$ would not be restricted to values smaller than 2. The family of the d-dimensional Sierpinski gaskets is a typical example, where by increasing the « control » parameter $\delta = d+3$, a qualitative change in the spectrum is observed. At $d = 1$, we have an absolutely continuous spectral measure, whereas for $d > 1$ the geometry of the gaskets, though regular, is able by itself to localize an important fraction of states, in the absence of any disorder. Such behaviour is to be compared with that of standard Euclidean lattices. A similar situation occurs in other regular systems like the spectrum of the almost-Mathieu equation [1]. It would be interesting to find in this case, scaling properties of the spectrum, if they exist at the critical point. It will also be useful to describe the nature of the eigenmodes at this point : extended chaotic [21] states or hierarchical states ? Finally, a spectrum qualitatively similar to that of the gaskets was recently observed in the quantum percolation problem [27]. This observation is consistent with the fractal structure of the percolation clusters.

Acknowledgments.

Helpful discussions with Drs. G. Toulouse and B. Souillard are gratefully acknowledged. We also thank Dr. R. Maynard for a critical reading of the manuscript and constructive suggestions. We are indebted to Professor S. Alexander for very useful comments, friendly correspondence about this work and for inspiring discussions. We also thank the referee of this paper for useful remarks and constructive suggestions.

Appendix I.

Recursion equation $\alpha' = \phi(\alpha)$ in the general d-dimension case. — The generalization of equation 2.7 to arbitrary d is not difficult. We give the main steps for the derivation of the recursion relation $\alpha' = \phi(\alpha)$ in this appendix. Without loss of generality we will assume d is even. Let consider a site common to two hypertetrahedrons, like X_0 in figure 12. On each of these two hypertetrahedrons, there are $(d + 1)$ sites of type X_0 : X_0 and $X_1, X_2, \ldots, X_d$ (resp. $Z_0 = X_0$ and $Z_1, Z_2, \ldots, Z_d$). At the mid points of the edges (X_0, X_i) the corresponding $d(d + 1)/2$ sites are denot-

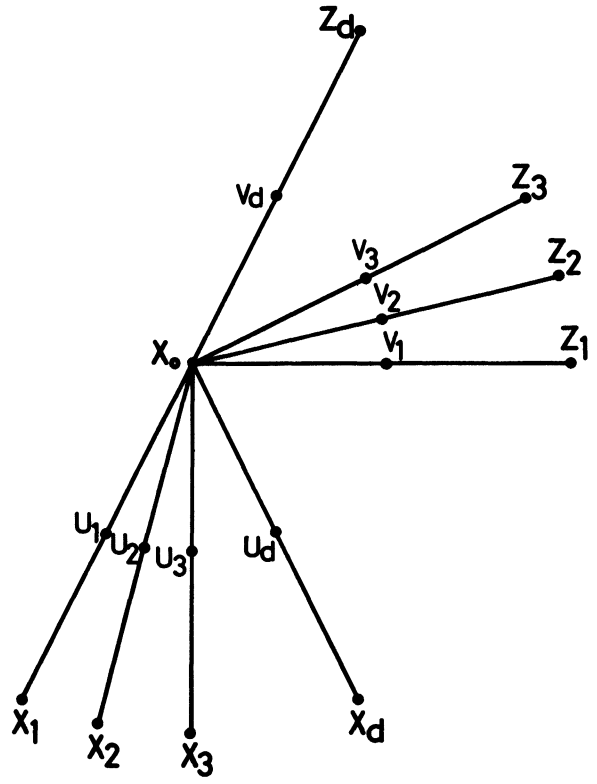

Fig. 12. — Neighbouring sites of an original site X_0 on a d-dimensional Sierpinski gasket.

ed by u_i (resp. v_i). Site X_0 is then connected to d sites of type u and each site u_i is connected to d neighbouring sites : 2 of type X and $(2\,d - 2)$ of type u. Finally, the total number of springs between u's is : $(d - 1)\,(d + 1)\,d/2$. The equation of motion at X_0 is written as

$$\alpha X_0 = \sum_{i=1}^{d} (X_0 - u_i) + \sum_{i=1}^{d} (X_0 - v_i). \quad \text{(A.1)}$$

For sites $\{ u_i \}$, we write similarly, with obvious notations

$$\begin{aligned} \alpha u_1 &= (u_1 - X_0) + (u_1 - X_1) + \sum_k (u_1 - u_k) \\ \alpha u_d &= (u_d - X_0) + (u_d - X_d) + \sum_k (u_d - u_k) \end{aligned} \quad \text{(A.2)}$$

and

$$\alpha u_k = (u_k - X) + (u_k - X') + \sum_j (u_k - u_j), \quad (d + 1) \leqslant k \leqslant d(d + 1)/2 \quad \text{(A.3)}$$

In equation A.3, X and X' denote the two neighbouring sites of type X. Let us define

$$U = \sum_{k=1}^{d} u_k, \quad U' = \sum_{k=d+1}^{d(d+1)/2} u_k \quad \text{(A.4)}$$

(similar definitions for V and V'), and add equations A.2 together :

$$\alpha U = 2\,\mathrm{d}U - (\mathrm{d}X_0 + X_1 + \cdots + X_d) - (d - 1)\,U - 2\,U' \quad \text{(A.5}a\text{)}$$

When equations A.2, A.3 are added, one obtains

$$\alpha(U + U') = 2(U + U') - \mathrm{d}(X_0 + X_1 + \cdots + X_d). \quad \text{(A.5}b\text{)}$$

The expressions of U and U' can be extracted from equations A.5a, A.5b. For instance :

$$U = X_0\left(-d + \frac{2\,d}{\alpha - 2}\right)\Big/(\alpha - (d + 3)) + \left(\frac{2\,d}{\alpha - 2} - 1\right)(X_1 + \cdots + X_d)/(\alpha - (d + 3)). \quad \text{(A.6)}$$

Analogous expressions can be written for V and V'. When (A.6) is replaced in (A.1), one obtains

$$\alpha X_0 = \left[2\,d - 2\,\frac{-d + \dfrac{2\,d}{\alpha - 2}}{\alpha - (d + 3)}\right] X_0 - \left[\frac{\dfrac{2\,d}{\alpha - 2} - 1}{\alpha - (d + 3)}\right](X_1 + \cdots + X_d + Z_1 + \cdots + Z_d). \quad \text{(A.7)}$$

The last equation is of the same form as (A.1), except the parameter α which is renormalized as

$$\alpha \to \alpha' = 2\,d - \frac{(\alpha - 2\,d)\,(\alpha - d - 3)\,(\alpha - 2) + 2[-d(\alpha - 2) + 2\,d]}{\alpha - 2 - 2\,d} \quad \text{(A.8)}$$

leading to

$$\alpha' = \alpha(\delta - \alpha) \equiv \phi(\alpha) \quad \text{(A.9)}$$

where $\delta = d + 3$.

Equation A.8 shows that $\phi(\alpha)$ is a rational fraction. The reduction of this fraction into a simple polynomial function (A.9) comes from various symmetry properties of the gasket. The same calculations can be performed for anisotropic gasket (with three parameters α_1, α_2 and α_3 for instance at $d = 2$), where some symmetry properties are lost. In this case, the renormalized parameters $\phi_i(\{ \alpha_j \})$ become rational fractions, because $\{ \alpha_j \}$ occurs linearly in the equations of motion. Therefore, the most general form expected for $\phi(\alpha)$ is a rational fraction.

Appendix 2.

Labelling procedure [11]. — Starting from the lowest left corner of the gasket, a natural coding of sites is easily obtained with the following rules (we shall illustrate this coding at $d = 2$). Each up triangle (plaquette) is labelled on the gasket at stage n by a word of n elements $(x_1\, x_2\, x_3 \ldots x_n)$ where $x_i = 0$, 1 or 2 ($1 \leqslant i \leqslant n$) are recursively defined from stage n to stage $n + 1$ (Fig. 13). Every plaquette has three neighbouring ones, which labels are trivially found using the above coding. In this way, the sites of the gasket (beside external sites) are labelled with the two plaquette labels sharing the considered site. This one-to-one correspondence between plaquettes and words of n elements is the basic code of the gasket.

i) Two plaquettes p_1 and p_2 are adjacent if and only if coded as follows :

$$p_1 : x_0\, x_1 \ldots x_k\, y\overbrace{zz \ldots}^{l}, \quad l \geqslant 0$$

$$p_2 : x_0\, x_1 \ldots x_k\, zyy \ldots y$$

where x_i, y and z are elements of $\mathfrak{T} = \{ 0, 1, 2 \}$ and $x_k \neq y, z$.

The common site to p_1 and p_2 will be coded by the following n-word :

$$x_0\, x_1 \ldots x_k\, u\, \underbrace{33 \ldots 3}_{l}$$

where u is neither y nor z in $\mathfrak{T}$.

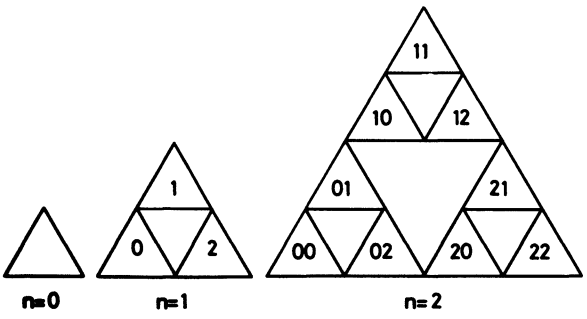

Fig. 13. — The Sierpinski gasket ($d = 2$) at successive stages : $n = 0$, 1 and 2. Stage $n + 1$ is obtained by the juxtaposition of three n-stage structures. For $n = 1$ and $n = 2$, we have shown the labelling of plaquettes (up triangles) used in the sites coding.

Inversely, a site coded by :

$$x_0\, x_1 \ldots x_k\, u\, \underbrace{33 \ldots 3}_{l}$$

is the common site to the following two plaquettes :

$$x_0\, x_1 \ldots x_k\, \underbrace{vww \ldots w}_{l}$$

and

$$x_0\, x_1 \ldots x_k\, wvv \ldots v$$

where $\{ u, v, w \} = \mathfrak{T}$.

ii) Rules for neighbouring sites : let $x_0\, x_1 \ldots x_k\, u\, 33 \ldots 3$, a given site on the gasket. In order to find the four nearest neighbouring sites ($n.n$), two cases are to be considered.

a) $l = 0$ ($k = n - 1$) : the two first $n.n$ sites are given by

$$x_0\, x_1 \ldots x_k\, v$$

and

$$x_0\, x_1 \ldots x_k\, w$$

where $\{ u, v, w \} = \mathfrak{T}$. The two others $n.n$ are :

$$x_0\, x_1 \ldots x_j\, yzz \ldots z$$

and

$$x_0\, x_1 \ldots x_j\, zyy \ldots y$$

where $j (\leqslant k)$ denotes the first integer (from the right) such that $x_j \neq u$ and $\{ x_{j+1}, y, z \} = \mathfrak{T}$.

b) $l \neq 0$: no $n.n$ site has « 3 » in its code, and the considered site is coded as follows :

$$x_0\, x_1 \ldots x_k\, u\, \underbrace{33 \ldots 3}_{l}.$$

The corresponding neighbouring sites are given by :

$$x_0\, x_1 \ldots x_k\, vuww \ldots w$$

$$x_0\, x_1 \ldots x_k\, vwuu \ldots u$$

$$x_0\, x_1 \ldots x_k\, wuvv \ldots v$$

and

$$x_0\, x_1 \ldots x_k\, wvuu \ldots u$$

where $\{ u, v, w \} = \mathfrak{T}$.

It is clear that the above coding is easily extended to dimensions $d = 3, 4, \ldots$ The set $\mathfrak{T}$ becomes $\mathfrak{T} = \{ 0, 1, 2, \ldots, d + 1 \}$, and the corresponding labelling procedure follows the same scheme illustrated above.

References

[1] AUBRY, S. and ANDRÉ, G., *Ann. Israel Phys. Soc.* **3** (1980) 111.

[2] GEFEN, Y., AHARONY, A., MANDELBROT, B. B. and KIRKPATRICK, S., *Phys. Rev. Lett.* **47** (1981) 1771.

[3] VOSS, R. F., LAIBOWITZ, R. B. and ALLESSANDRINI, E. I., *Phys. Rev. Lett.* **49** (1982) 1441.
KAPITULNIK, A. and DEUTSCHER, G., *Phys. Rev. Lett.* **49** (1982) 1444.

[4] MANDELBROT, B. B., *Fractals : Form, Chance and Dimension* (Freeman, San Francisco) 1977.

[5] ALEXANDER, S. and ORBACH, R., *J. Phys. Lett.* **43** (1982) L-625.

[6] RAMMAL, R. and TOULOUSE, G., *J. Phys. Lett.* **44** (1983) L-13.

[7] RAMMAL, R. and TOULOUSE, G., *Phys. Rev. Lett.* **49** (1982) 1194.

[8] ALEXANDER, S., *Phys. Rev. B* **27** (1983) 1541.

[9] BACHMAN, G., *Introduction to p-adic Numbers and valuation theory* (Academic New York) 1964.

[10] MAHLER, K., *p-adic numbers and their functions* (Cambridge University Press, England) 1973.

[11] ANGLES D'AURIAC, J. C., BENOIT, A. and RAMMAL, R., *J. Phys. A* **16** (1983) in press.

[12] JULIA, G., *J. Math. Pures Appl.* (Ser. 8) **1** (1918) 47.

[13] FATOU, P., *Bull. Soc. Math.* **47** (1919) 161 ; **48** (1920) 33 and 208.

[14] BROLIN, H., *Arkiv Matematik* **6** (1965) 103.

[15] DOMANY, E., ALEXANDER, S., BENSIMON, D. and KADANOFF, L. P. (1983) (to be published).

[16] EDWARDS, S. F. and JONES, R. C., *J. Phys. A* **9** (1976) 1595.
SCHEMELTZER, D. and BESERMAN, R., *Phys. Rev. B* **22** (1980) 6330.

[17] MARADUDIN, A. A., MONTROLL, E. W. and WEISS, G., *Theory of lattice dynamics in the harmonic approximation*, Ed. F. Seitz and D. Turnbull (Academic Press, New York) 1963.

[18] DHAR, D., *J. Math. Phys.* **18** (1977) 577.

[19] MONTEL, P., *Leçons sur les récurrences et leurs applications* (Gauthier-Villard, Paris) 1957.

[20] KUCZMA, M., *Functional equations in a single variable*, Warszawa (PWN Polish Sci. Publ.) 1968.

[21] BELLISSARD, J., BESSIS, D. and MOUSSA, P., *Phys. Rev. Lett.* **49** (1982) 701.

[22] BESSIS, D., MEHTA, M. L. and MOUSSA, P., *Lett. Math. Phys.* **6** (1982), 123. See also BESSIS, D. and MOUSSA, P., *Commun. Math. Phys.* **88** (1983) 503 and BARNSLEY, M. F., GERONIMO, J. S. and HARRINGTON, A. N., *Comm. Math. Phys.* **88** (1983) 479.

[23] POLYA, G. and SZEGÖ, *Problems and theorems in Analysis* (Springer, Berlin) 1972, vol. 1.

[24] BERRY, M. V., in *Proc. Tübingen Symp. honouring R. Thom*, Ed. Güttinger (Springer, Berlin) 1979, 51.

[25] KAC, M., *Am. Math. Month.* **73** (1966) 1.

[26] HEIJHAL, D. A., *Duke Math. J.* **43** (1976) 441.
MCKEAN, Jr. H. P. and SINGER, T. M., *J. Diff. Geom.* **1** (1967) 43.

[27] SHAPIR, Y., AHARONY, A. and HARRIS, A. B., *Phys. Rev. Lett.* **49** (1982) 486.